Cell Reports
Report

Hebbian Plasticity Guides Maturation of Glutamate Receptor Fields In Vivo

Dmitrij Ljaschenko,[1] Nadine Ehmann,[1] and Robert J. Kittel[1,*]
[1]Institute of Physiology, Department of Neurophysiology, University of Würzburg, 97070 Würzburg, Germany
*Correspondence: robert.kittel@uni-wuerzburg.de
http://dx.doi.org/10.1016/j.celrep.2013.04.003

SUMMARY

Synaptic plasticity shapes the development of functional neural circuits and provides a basis for cellular models of learning and memory. Hebbian plasticity describes an activity-dependent change in synaptic strength that is input-specific and depends on correlated pre- and postsynaptic activity. Although it is recognized that synaptic activity and synapse development are intimately linked, our mechanistic understanding of the coupling is far from complete. Using Channelrhodopsin-2 to evoke activity in vivo, we investigated synaptic plasticity at the glutamatergic *Drosophila* neuromuscular junction. Remarkably, correlated pre- and postsynaptic stimulation increased postsynaptic sensitivity by promoting synapse-specific recruitment of GluR-IIA-type glutamate receptor subunits into postsynaptic receptor fields. Conversely, GluR-IIA was rapidly removed from synapses whose activity failed to evoke substantial postsynaptic depolarization. Uniting these results with developmental GluR-IIA dynamics provides a comprehensive physiological concept of how Hebbian plasticity guides synaptic maturation and sparse transmitter release controls the stabilization of the molecular composition of individual synapses.

INTRODUCTION

The ability of chemical synapses to change their structural, functional, and molecular properties in an activity-dependent manner has attracted considerable scientific interest over the past few decades (Kandel, 2009). Originally put forward as a theory by Donald O. Hebb (Hebb, 1949), today the term "Hebbian synaptic plasticity" commonly describes a change in synaptic strength that depends on correlated pre- and postsynaptic neuronal activity and acts independently at individual synapses. Thus, Hebbian plasticity represents a powerful synaptic learning rule that provides an attractive subcellular mechanism for models of neuronal network formation, learning, and memory (Abbott and Nelson, 2000). Descriptions of synaptic long-term potentiation (LTP) and long-term depression (LTD) have provided experimental examples of Hebbian plasticity and emphasized the pivotal role of the temporal order of pre- and postsynaptic activity in determining the polarity of synaptic changes (i.e., potentiation or depression; Feldman, 2012).

The excellent genetic accessibility of the glutamatergic *Drosophila* neuromuscular junction (NMJ) has contributed to its popularity as an experimental system for identifying the molecular mechanisms that govern synaptic function (Bellen et al., 2010). Due to its rapid growth, the larval NMJ exhibits a high degree of developmental synaptic plasticity. Positive and negative feedback loops operate on neuronal structure and presynaptic function in a manner that appears to depend on the duration and site of the activity alteration. Elevated motorneuron activity promotes the growth of neuromuscular boutons (Ataman et al., 2008; Budnik et al., 1990; Sigrist et al., 2003), and both decreased postsynaptic and increased presynaptic excitation facilitate transmitter release from active zones (DiAntonio et al., 1999; Frank et al., 2006; Paradis et al., 2001; Sigrist et al., 2003; Steinert et al., 2006).

The application of in vivo imaging at the *Drosophila* NMJ has provided valuable information about the developmental maturation of synapses in an intact organism (Rasse et al., 2005; Schmid et al., 2008). During this process, non-NMDA-type ionotropic glutamate receptors (GluRs) assemble as heterotetramers of GluR-IIC/III, IID, and IIE subunits plus either GluR-IIA or GluR-IIB (Featherstone et al., 2005; Marrus et al., 2004; Qin et al., 2005). These two receptor complexes differ markedly in their physiological parameters: GluR-IIB-type receptors desensitize far more rapidly than receptors containing GluR-IIA (DiAntonio et al., 1999). At individual synapses, receptor fields initially grow by incorporating GluR-IIA-type receptors. As the corresponding presynaptic active zone matures, incorporation then shifts toward GluR-IIB, until an even ratio of IIA and IIB is reached at mature synapses (Schmid et al., 2008). A mechanistic understanding of synapse development will require identification of the physiological cues that guide such molecular dynamics. Although at present the identity of these cues remains largely elusive, several lines of evidence indicate that synaptic activity itself is highly influential.

Whereas the total number of receptors is largest opposite active zones that possess a high neurotransmitter release probability, p_r (Marrus and DiAntonio, 2004), the relative contribution of GluR-IIA is highest opposite low-p_r sites (Schmid et al., 2008). These observations are consistent with subunit dynamics during synapse development and suggest a form of synaptic scaling, i.e., a compensatory effect exerted by the large current-passing

Cell PRESS
Open ACCESS

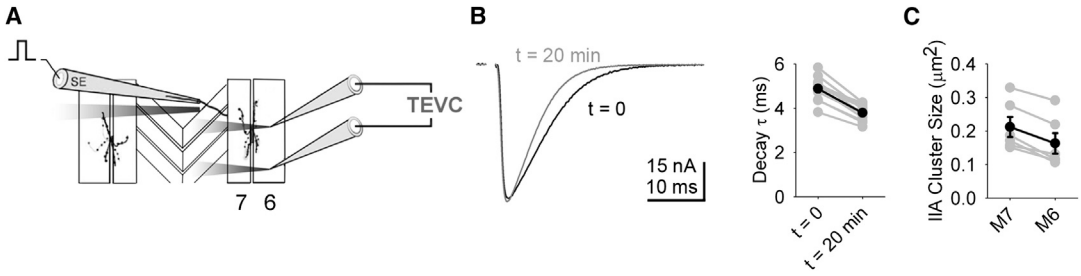

Figure 1. Activity-Dependent GluR-IIA Removal from PSDs

(A) TEVC recordings were made from M6 during electrical stimulation (0.2 Hz) of the nerve innervating M6 and M7 via a suction electrode (SE; modified from Pawlu et al., 2004).

(B) Representative traces (black, t = 0 min; gray, t = 20 min) and data summary (gray, individual recording; black, mean value) demonstrate the significant stimulus-induced reduction of eEJC decay τ.

(C) Staining against GluR-IIA revealed smaller receptor clusters on M6 compared with the adjacent M7 after 20 min of stimulation. Error bars represent SEM.

capacity of GluR-IIA. However, taking chronic changes in neuronal activity into account produces a more complex picture, as sustained increases in neuronal activity, induced either genetically or through elevated locomotion, globally raise synaptic GluR-IIA levels (Sigrist et al., 2000, 2003).

Our goal in this study was to improve our mechanistic understanding of how activity-dependent synaptic plasticity is linked to the development of glutamatergic synapses. To this end, we employed optogenetics at the developing larval *Drosophila* NMJ. We chose to use Channelrhodopsin-2 (ChR2; Nagel et al., 2003) because this enabled us to induce cellular activity in vivo in an acute, quantifiable manner and direct it solely at pre- or postsynaptic compartments, or at both compartments simultaneously. Focusing on postsynaptic GluRs, our results unveil a Hebbian mode of GluR-IIA incorporation at postsynaptic sites that is counteracted by GluR-IIA removal when synaptic transmission fails to evoke considerable muscle depolarization. We report rapid receptor mobilization rates that were previously undetected by in vivo time-lapse imaging (Rasse et al., 2005; Schmid et al., 2008) and provide a comprehensive physiological picture of how activity-dependent plasticity controls the molecular maturation and stabilization of individual synapses.

RESULTS

Rapid GluR Removal from Synapses

In two-electrode voltage clamp (TEVC) recordings from larval *Drosophila* NMJs (Figure 1A), we observed a kinetic change of synaptic currents during low-frequency nerve stimulation. Specifically, the decay time constant (τ_{decay}) of evoked excitatory junctional currents (eEJCs) decreased within 20 min (Figure 1B; τ_{decay} at t = 0: 4.99 ± 0.14 ms; t = 20 min: 3.86 ± 0.10; n = 10, p < 0.001 paired t test). The proportion of slowly desensitizing IIA-type GluRs in postsynaptic densities (PSDs) correlates with the length of the τ_{decay} of synaptic currents (Schmid et al., 2008). To examine whether the electrophysiological signature correlated with the molecular composition of PSDs, NMJs were stained against GluR-IIA. Following nerve stimulation, GluR-IIA clusters were significantly smaller in voltage-clamped muscle 6 (M6) compared with its neighboring muscle, M7 (Figure 1C; M7: 0.212 ± 0.030 μm^2; M6: 0.163 ± 0.031 μm^2; n = 6, p = 0.001 paired t test). M6 and M7 are innervated by the same motorneurons. Because the membrane potential of only M6 was held constant, these results indicate that preventing postsynaptic depolarization during neurotransmission drove GluR-IIA out of PSDs (there was no difference in the average GluR-IIA cluster size between M6 and M7 on the contralateral, unstimulated side; p = 0.495 paired t test, data not shown).

Such rapid GluR mobilization has not previously been observed during the development of this synaptic system in vivo (Rasse et al., 2005; Schmid et al., 2008). We therefore employed ChR2 to obtain a better understanding of the specific role of activity in controlling GluR dynamics in the intact organism.

Quantification of ChR2 Expression and Activity

To attain independent functional control over pre- and postsynaptic compartments, we employed the bipartite Gal4/UAS system (Brand and Perrimon, 1993) for tissue-specific expression of ChR2 (Schroll et al., 2006). Specifically, ChR2 was driven presynaptically in motorneurons (*ok6-gal4* > *UAS-chop2*; "Pre"), postsynaptically in muscles (*g7-gal4* > *UAS-chop2*; "Post"), or in both compartments simultaneously (*ok6-gal4* & *g7-gal4* > *UAS-chop2*; "Pre & Post"; Figure 2A). Genetically expressed channelopsin-2 (Chop2) requires addition of its chromophore all-*trans*-retinal (RAL) to deliver functional ChR2 (Nagel et al., 2003). Raising *Drosophila* larvae under standard conditions (defined here as 25°C and 0.1 mM RAL food supplement) yielded the expected distributions of ChR2 immunoreactivity (Figure S1). TEVC recordings were employed to measure photocurrents. Activation of ChR2 in motorneurons (Pre) elicited light-evoked EJCs (lEJCs), activation in muscles gave rise to postsynaptic steady-state currents (Post), and combined activation (Pre & Post) produced composite photocurrents (Figure S2).

Activity-Induced Functional Synaptic Plasticity In Vivo

To test for activity-dependent induction of synaptic plasticity, we subjected fully intact, freely moving larvae to light stimulation (peak ~460 nm; Figure S3A), which evoked visible muscle contractions in vivo (Figure 2B). Based on the quantification of ChR2 function (Figure S2), we chose an intermediate irradiance (1.7 mW/mm^2 at 460 nm; also for all subsequent experiments), and applied the light according to an established protocol under

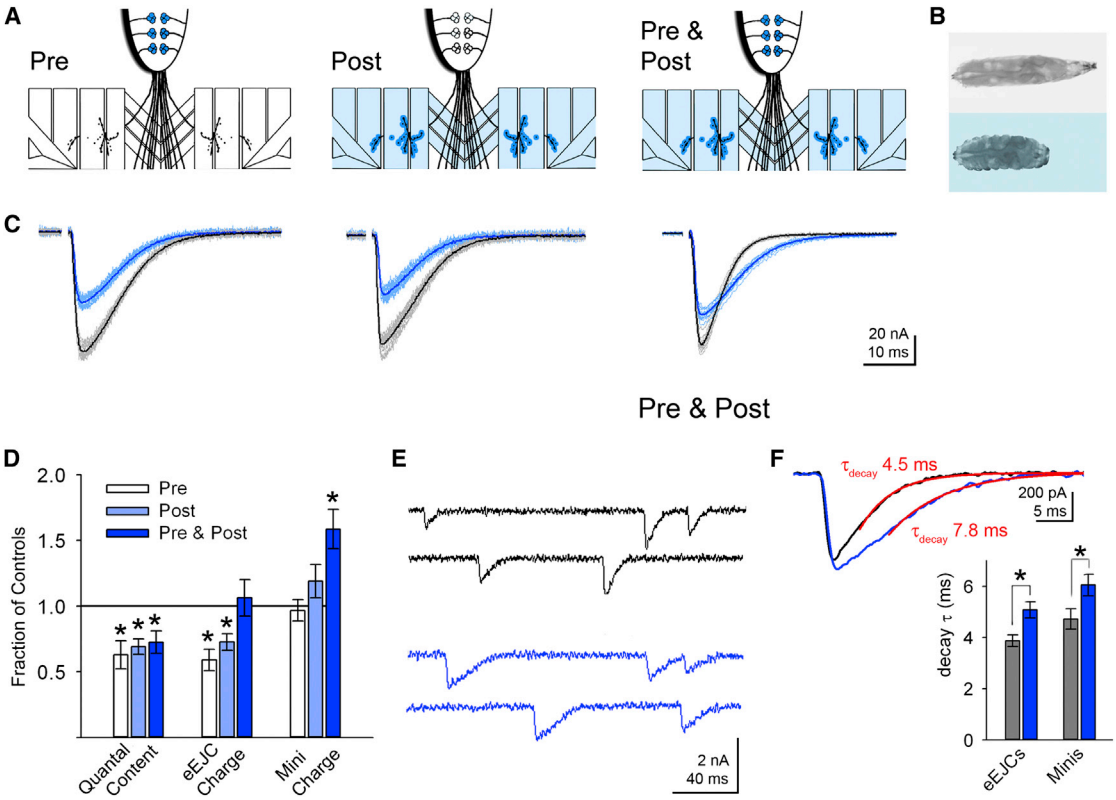

Figure 2. Tissue-Specific Expression of ChR2 and Induction of Functional Synaptic Plasticity In Vivo

(A) Schematic illustration of ChR2 localization based on antibody stainings (Figure S1). ChR2 expression was driven in presynaptic motorneurons (Pre), in postsynaptic muscles (Post), or in both compartments (Pre & Post).

(B) Example of light-induced muscle contractions in a Pre larva.

(C) Representative TEVC recordings of eEJCs following activity induction in vivo. Individual traces (light) overlaid with mean (dark) for RAL-fed (blue) and control (gray) groups of the indicated genotypes. Stimulation artifacts have been removed for clarity.

(D) Relative change of mean quantal content, eEJC charge, and mini charge in RAL-fed larvae (white, Pre; light blue, Post; dark blue, Pre & Post) compared with their respective controls.

(E and F) Representative recordings of minis at Pre & Post (blue) and control (black) NMJs (E), and examples of averaged minis (F). The τ_{decay} of both eEJCs and minis was significantly prolonged at Pre & Post NMJs (blue) compared with controls (gray). Error bars represent SEM.

See also Figure S3.

standard conditions, though likely with higher light intensity than previously reported (Figure S3B; Movie S1; Ataman et al., 2008). Following the 100-min-long protocol, the larvae were dissected for synaptic structure-function analyses. Importantly, the dependence of functional ChR2 on RAL enabled us to use larvae that were not fed RAL as controls. These larvae were of the same genotype as the respective experimental groups and were also subjected to light stimulation. Hence, the experiments measured effects that were specifically mediated by ChR2 function and could not be attributed to the genetic background or an unspecific influence of light application. Correspondingly, lEJCs could not be triggered when RAL was omitted, and the controls of all three genotypes failed to display light-induced muscle contractions during application of the plasticity protocol (data not shown).

In all three genotypes, neither the NMJ size nor the numbers or average sizes of presynaptic active zones (recognized by the central active zone protein Bruchpilot [BRP]; Wagh et al., 2006) or postsynaptic receptor fields (identified via the universal GluR-IID subunit) were influenced by light stimulation in vivo (Figures S4A–S4C; Table S1). In contrast, electrophysiological recordings revealed pronounced activity-induced functional changes (Figures 2C–2F; Table S2). Solely pre- or postsynaptic or combined activation of ChR2 in vivo led to a significant reduction in the number of vesicles released from active zones per action potential (quantal content; Figure 2D; Pre control: 105 ± 13 vesicles, n = 10 NMJs, Pre RAL: 66 ± 11 vesicles, n = 10, p = 0.021 rank sum test (rs test); post control: 98 ± 6 vesicles, n = 11, post RAL: 68 ± 6 vesicles, n = 11, p = 0.002 t test; Pre & post control: 150 ± 10 vesicles, n = 11 NMJs, Pre & post RAL: 109 ± 13 vesicles, n = 10, p = 0.02 t test).

Crucially, a second form of plasticity was induced specifically by combined pre- and postsynaptic ChR2 stimulation. This was manifested in a kinetic change of currents evoked by action potentials and spontaneous single-vesicle fusions (minis; Figures 2C–2F; Table S2; control eEJCs τ_{decay} 3.87 ± 0.23 ms, n = 11 NMJs, Pre & Post eEJCs τ_{decay} 5.08 ± 0.32 ms, n = 10, p = 0.006 t test; control minis τ_{decay} 4.72 ± 0.40 ms, n = 11,

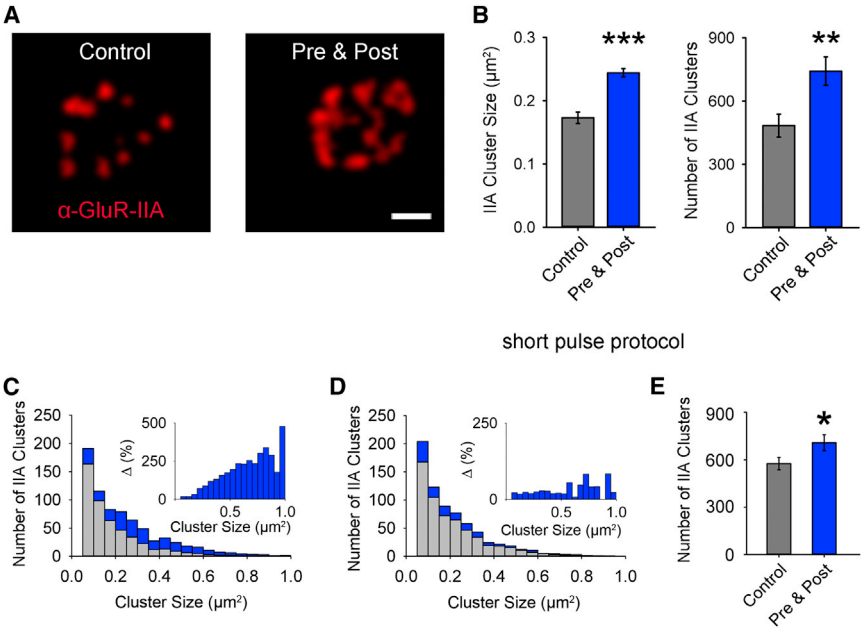

Figure 3. Correlated Activity Drives Selective Incorporation of GluR-IIA into PSDs

(A) Representative stainings of GluR-IIA clusters (red).

(B) Quantification of GluR-IIA clusters. After ChR2 stimulation (standard protocol, 2 s pulses), GluR-IIA clusters were significantly increased in size and number at Pre & Post NMJs (blue) compared with controls (gray).

(C and D) Mean distributions of GluR-IIA cluster sizes at Pre & Post NMJs (blue) following stimulation with the standard protocol or with the short pulse protocol (controls in gray; Figure S5). Insets show relative change in receptor numbers (Δ).

(E) Compared with controls, more GluR-IIA clusters were detected at Pre & Post NMJs following brief paired stimulation. Scale bar, 1 μm. Error bars represent SEM.

Pre & Post minis τ_{decay} 6.05 ± 0.42 ms, n = 11, p = 0.01 rs test). The protraction of minis produced a substantially larger quantal charge (~60% increase; Table S2), which in turn gave rise to a normal compound charge transfer (control eEJCs: 483 ± 52 pC, n = 11 NMJs; Pre & Post eEJCs: 514 ± 67 pC, n = 10; p = 0.504 rs test) despite the reduced quantal content. Hence, correlated pre- and postsynaptic activity gave rise to functional plasticity at the level of quantal transmission.

Connecting Synaptic Structure and Function

Motivated by the causal link between rapid current decay and low synaptic GluR-IIA levels (Figures 1B and 1C; DiAntonio et al., 1999; Schmid et al., 2008), we examined the receptor subunit composition of Pre & Post PSDs. In agreement with the electrophysiological data, NMJs subjected to correlated pre- and postsynaptic activity displayed more GluR-IIA clusters than the unstimulated controls (Figure 3B; control 481 ± 54 clusters, n = 25 NMJs; Pre & Post 742 ± 67 clusters, n = 21, p = 0.002 rs test). Furthermore, this effect was accompanied by a significant increase in the average size of GluR-IIA accumulations (Figures 3A–3C; control 0.173 ± 0.009 μm^2, n = 25 NMJs; Pre & Post 0.244 ± 0.007 μm^2, n = 21, p < 0.001 t test). In contrast, neither the number (control 472 ± 21 clusters, n = 30 NMJs; Pre & Post 523 ± 28 clusters, n = 29; p = 0.152 t test) nor the average size of the GluR-IIB clusters (Figures S4D and S4E; control 0.140 ± 0.003 μm^2, n = 30 NMJs; Pre & Post 0.150 ± 0.005 μm^2, n = 29; p = 0.063 t test) were significantly influenced by activity. Thus, combined pre- and postsynaptic stimulation led to a specific increase of GluR-IIA-containing receptors in PSDs.

Correlative Activity Triggers GluR-IIA Incorporation

The combined depolarization of motorneuron and muscle evoked more current flow over the postsynaptic membrane than did isolated pre- or postsynaptic activation. Thus, we set out to test whether GluR-IIA-mediated synaptic plasticity was caused merely by stronger stimulation or instead reflected the correlative nature of combined pre- and postsynaptic activation. To this end, we reduced the light pulse duration from 2 s to 15 ms (Figure S5C) while preserving the correlative property of the stimulation (Figures S5A and S5B). Briefly synchronized pre- and postsynaptic activity in vivo did not produce a change in quantal content or current decay (Figure S5D). However, the number of GluR-IIA clusters increased from 576 ± 39 in controls (n = 25 NMJs) to 708 ± 51 in Pre & Post larvae (n = 17, p = 0.045 t test; Figure 3E). Hence, briefly correlated pre- and postsynaptic activity was sufficient to increase GluR-IIA levels in PSDs. Plotting the distribution of GluR-IIA cluster sizes (Figure 3D) illustrates that short pulses led to a uniform increase in the number of clusters (stable mean cluster size), whereas long light pulses produced bigger average clusters (Figure 3B) by generating a greater increase in the number of large clusters (Figure 3C).

GluR-IIA Incorporation Is Synapse Specific

In addition to its correlative quality, a defining feature of Hebbian plasticity is its synapse-specific action (Abbott and Nelson, 2000; Hebb, 1949). In order to examine whether GluR-IIA-mediated synaptic plasticity met this criterion at the NMJ, we again expressed ChR2 in motorneurons but this time in combination with a GAL4 line that drives expression only in M12 (Figures 4A and S6). This enabled us to compare activity-induced effects on synapses that experienced either solely presynaptic or combined pre- and postsynaptic stimulation. The analyzed synapses are in close proximity to each other and are formed by both shared and unique motorneurons (Hoang and Chiba, 2001). Hence, this experimental setup provided an ideal internal control for variations arising from differences between individuals.

Larvae (Pre & M12-Post) were subjected to the short-pulse protocol in vivo. In control animals, GluR-IIA clusters were significantly smaller in M12 than in the adjacent M13 (M12: 0.195 ± 0.007 μm^2; M13: 0.214 ± 0.010 μm^2; n = 18, p = 0.011 paired

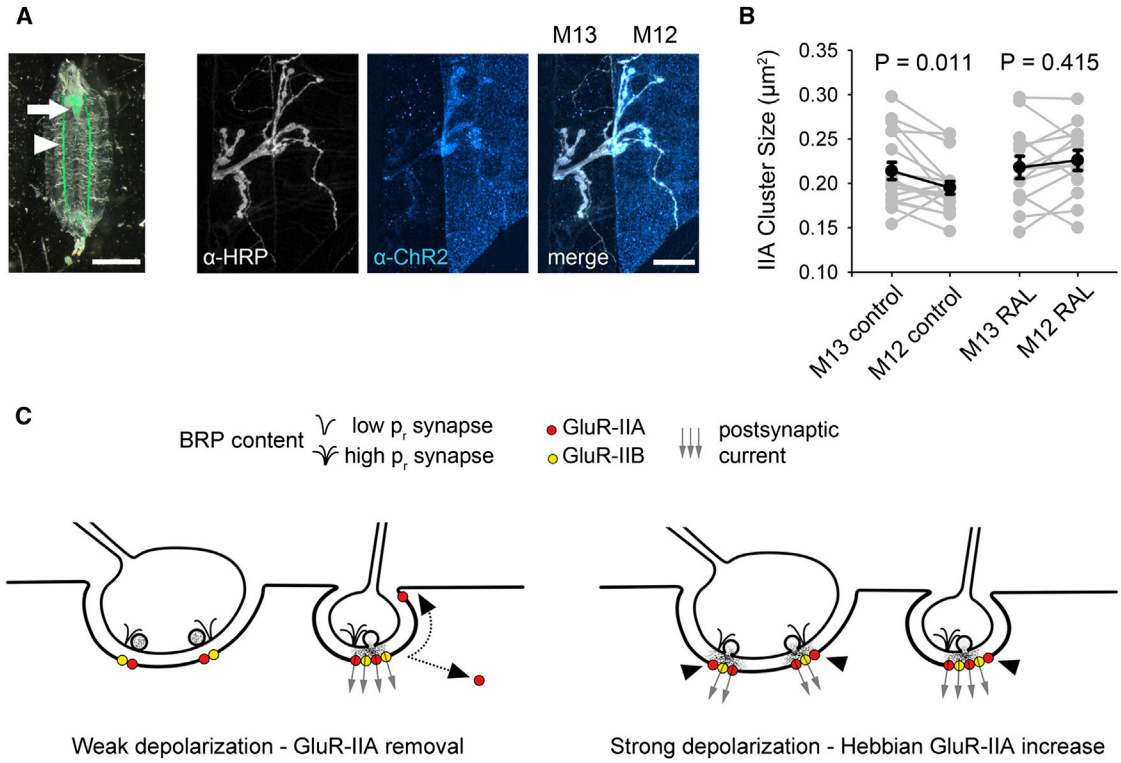

Figure 4. Input-Specific Induction of Hebbian Synaptic Plasticity Completes a Comprehensive Mechanism of Activity-Dependent Receptor Dynamics

(A) Dissected larva expressing EGFP under control of *ok6-gal4 & m12-gal4* (arrow indicates CNS, arrowhead points to M12). Double staining against HRP (gray) and ChR2 (blue) at Pre & M12-Post NMJs of M12 and M13 (Figure S6). Scale bars, 1 mm (left) and 20 μm (right).

(B) Comparison of GluR-IIA cluster sizes on M12 and M13 following the short-pulse protocol in control and RAL-fed Pre & M12-Post larvae. Adjacent muscles are connected by a line (gray, individual larvae; black, mean values). GluR-IIA clusters were significantly smaller on M12 than on M13 in controls, but attained an equal size in RAL-fed Pre & M12-Post larvae after the short-pulse protocol. Error bars represent SEM.

(C) Model of activity-dependent GluR-IIA dynamics. Sparse activity occurring only at high-p_r active zones (high BRP content) induces only weak muscle depolarization and triggers synapse-specific GluR-IIA exit (dotted lines). Synchronized synaptic exocytosis induces strong muscle depolarization and triggers Hebbian GluR-IIA incorporation at all active synapses (arrowheads).

t test; Figure 4B). However, when synapses on M12 repeatedly experienced correlated pre- and postsynaptic stimulation, their size was selectively increased compared with synapses on M13, which had received only presynaptic stimulation and showed no increase in size (M12: 0.226 ± 0.011 μm^2; M13: 0.218 ± 0.013 μm^2; n = 13, p = 0.415 paired t test; Figure 4B). These results support a synapse-specific mechanism of correlative plasticity that acts locally enough to discriminate between synapses formed on adjacent muscles.

DISCUSSION

Activity-Induced Plasticity

Repeated light-triggered neurotransmitter release from presynaptic active zones provoked synaptic depression via a decrease in quantal content. Interestingly, muscle depolarization itself also led to a drop in quantal content despite bypassing synapses (Post animals). The latter observation is highly reminiscent of homeostatic communication whereby a retrograde pathway of inverted polarity operates to increase quantal content in response to reduced muscle excitability (DiAntonio et al., 1999; Frank et al., 2006; Paradis et al., 2001). Future studies can now test whether molecular components involved in the homeostatic upregulation of quantal content (Dickman and Davis, 2009) also contribute to its downregulation following postsynaptic ChR2 stimulation.

Pairing pre- and postsynaptic depolarizations repetitively (Pre & Post) triggered a synapse-specific increase in postsynaptic GluR-IIA-type GluRs. Hence, correlated activity initiated a Hebbian form of synaptic plasticity at the *Drosophila* NMJ. A comparison of the cluster size distributions following brief and long pulses (Figures 3C and 3D) suggests two phases of plasticity. The first phase of activity-induced plasticity (15 ms pulses) promotes an evenly distributed increase in the number of clusters. Therefore, despite an increase in total number, the average size of GluR-IIA clusters is not significantly altered. The next phase (2 s pulses) then leads to an increase mainly in the number of large clusters, and hence the average GluR-IIA cluster size increases (Figure 3B). Neurotransmitter p_r varies across active zones at the NMJ (Peled and Isacoff, 2011). Because the size of GluR clusters is largest opposite high-p_r active zones (Marrus and DiAntonio, 2004), it is to be expected that functional

recordings of synaptic currents preferentially sample large receptor fields. For this reason, GluR-IIA incorporation likely remained below the detection threshold in electrophysiological recordings following brief light pulses (Figure S5D).

In view of the unchanged total number of receptor fields (anti-GluR-IID staining) and active zones (Figure S4B), paired stimulation did not appear to give rise to the formation of new synapses. Instead, GluR-IIA was likely incorporated into receptor fields with previously undetectable IIA levels.

Linking Developmental and Activity-Dependent Synaptic Plasticity

In vivo imaging suggests that positive feedback initially promotes GluR-IIA incorporation during synapse growth and that GluR-IIA entry is specifically restrained with further maturation, whereas the rate of GluR-IIB recruitment remains constant (Schmid et al., 2008). The physiological signals that guide these synapse-specific molecular dynamics are unknown. We argue that the Hebbian mechanism identified in the present study represents the signal that promotes GluR-IIA entry during synapse development. This is consistent with the observed increase in small clusters following short pulses. Furthermore, in this framework, paired pre- and postsynaptic stimulation would be able to override the inhibition of GluR-IIA incorporation at relatively mature receptor fields (Figure 3C) and thereby restore the ''juvenile behavior'' of the PSDs.

At the developing *Drosophila* NMJ, receptor field growth is accompanied by BRP-dependent, active zone maturation (Schmid et al., 2008). Correspondingly, large receptor fields are found opposite high-p_r active zones that are rich in BRP (Marrus and DiAntonio, 2004). Therefore, small, growing receptor fields opposite immature, low-p_r active zones will tend to be exposed to glutamate only when p_r is elevated, e.g., during trains of action potentials. Because a large number of other synapses will also be active at these time points, transmitter release will coincide with strong postsynaptic depolarization, leading to Hebbian GluR-IIA incorporation.

A comprehensive model conversely demands a signal to remove GluR-IIA from mature receptor fields in order to describe their diminished rate of IIA incorporation in vivo and to limit receptor-field growth. We reason that such a physiological cue could be provided by sparse (i.e., unsynchronized) transmitter release that preferentially occurs at high-p_r, mature synapses and does not trigger substantial muscle depolarization. This hypothesis is experimentally supported by GluR-IIA removal from synapses when muscle depolarization is prevented during neurotransmission (Figure 1).

Here, we introduce a physiological model (Figure 4C) in which GluR-IIA is increased at simultaneously active synapses via Hebbian plasticity and is decreased at solitarily active synapses. Such solitary activity may be provided by spontaneous transmitter release (i.e., minis). The physiological function of minis has been controversially discussed (Verstreken and Bellen, 2002). Our results suggest that they contribute to ''taming the beast'' (Abbott and Nelson, 2000); in other words, restraining the extent of Hebbian plasticity. Our model can account for developmental, synapse-specific receptor subunit dynamics, and explains why GluR-IIA levels are higher opposite low-p_r Ib motorneurons than opposite high-p_r Is motorneurons (Schmid et al., 2008). This conceptual framework can account for an increase in GluR-IIA following chronic activity elevation (Sigrist et al., 2000, 2003) and is consistent with low synaptic IIA levels in the presence of ambient extracellular glutamate, although, intriguingly, sustained glutamate exposure also affects GluR-IIB (Augustin et al., 2007).

Trains of action potentials are likely the physiological equivalent of paired pre- and postsynaptic depolarization, which simply triggers the Hebbian change more efficiently than solely presynaptic ChR2 stimulation. Notably, rapid GluR-IIA exit can be acutely provoked (Figure 1). This observation is compatible with fast GluR dynamics in mammals, which can operate on a timescale of minutes and well below (Heine et al., 2008). Hence, rapid receptor trafficking also occurs in *Drosophila*, though this probably remains concealed when receptor exit is not explicitly provoked during time-lapse imaging of synapse development in vivo (Rasse et al., 2005; Schmid et al., 2008).

Perhaps most conspicuously, activity-dependent bidirectional GluR-IIA mobility is reminiscent of subunit-specific AMPA receptor trafficking at mammalian central synapses, which mediates manifold forms of synaptic plasticity (Malinow and Malenka, 2002). Local activity has been shown to drive synapse-specific accumulation of GluR1 AMPA receptors (Ehlers et al., 2007). Whereas high-frequency stimulation triggers LTP and synaptic GluR1 incorporation, low-frequency stimulation triggers LTD and GluR1 removal (Shepherd and Huganir, 2007). Collectively, these considerations support the notion that fundamental mechanisms of synaptic plasticity have been strongly conserved during evolution (Glanzman, 2010).

EXPERIMENTAL PROCEDURES

TEVC recordings, stainings, and image analysis were performed essentially as previously described (Schmid et al., 2008). For application of the activity protocol in vivo, freely moving larvae were stimulated with a blue LED. In the figures, the level of significance is marked with asterisks (*$p \leq 0.05$; **$p \leq 0.01$; ***$p \leq 0.001$). Detailed methods are available in Extended Experimental Procedures.

SUPPLEMENTAL INFORMATION

Supplemental Information includes Extended Experimental Procedures, six figures, two tables, and one movie and can be found with this article online at http://dx.doi.org/10.1016/j.celrep.2013.04.003.

LICENSING INFORMATION

ACKNOWLEDGMENTS

We thank G. Nagel and C. Stangl for supporting the irradiance measurements; E. Buchner, A. DiAntonio, A. Fiala, and S.J. Sigrist for providing fly stocks and reagents; U. Ashery, S. Hallermann, M. Heckmann, and T. Langenhan for scientific discussions; and C. Wirth for technical assistance. This work was supported by grants from the DFG (Emmy Noether KI 1460/1-1 to R.J.K.) and the GSLS, University of Würzburg (to N.E.).

Received: December 6, 2012
Revised: March 18, 2013
Accepted: April 3, 2013
Published: May 2, 2013

REFERENCES

Abbott, L.F., and Nelson, S.B. (2000). Synaptic plasticity: taming the beast. Nat. Neurosci. Suppl. *3*, 1178–1183.

Ataman, B., Ashley, J., Gorczyca, M., Ramachandran, P., Fouquet, W., Sigrist, S.J., and Budnik, V. (2008). Rapid activity-dependent modifications in synaptic structure and function require bidirectional Wnt signaling. Neuron *57*, 705–718.

Augustin, H., Grosjean, Y., Chen, K., Sheng, Q., and Featherstone, D.E. (2007). Nonvesicular release of glutamate by glial xCT transporters suppresses glutamate receptor clustering *in vivo*. J. Neurosci. *27*, 111–123.

Bellen, H.J., Tong, C., and Tsuda, H. (2010). 100 years of *Drosophila* research and its impact on vertebrate neuroscience: a history lesson for the future. Nat. Rev. Neurosci. *11*, 514–522.

Brand, A.H., and Perrimon, N. (1993). Targeted gene expression as a means of altering cell fates and generating dominant phenotypes. Development *118*, 401–415.

Budnik, V., Zhong, Y., and Wu, C.F. (1990). Morphological plasticity of motor axons in *Drosophila* mutants with altered excitability. J. Neurosci. *10*, 3754–3768.

DiAntonio, A., Petersen, S.A., Heckmann, M., and Goodman, C.S. (1999). Glutamate receptor expression regulates quantal size and quantal content at the *Drosophila* neuromuscular junction. J. Neurosci. *19*, 3023–3032.

Dickman, D.K., and Davis, G.W. (2009). The schizophrenia susceptibility gene dysbindin controls synaptic homeostasis. Science *326*, 1127–1130.

Ehlers, M.D., Heine, M., Groc, L., Lee, M.C., and Choquet, D. (2007). Diffusional trapping of GluR1 AMPA receptors by input-specific synaptic activity. Neuron *54*, 447–460.

Featherstone, D.E., Rushton, E., Rohrbough, J., Liebl, F., Karr, J., Sheng, Q., Rodesch, C.K., and Broadie, K. (2005). An essential *Drosophila* glutamate receptor subunit that functions in both central neuropil and neuromuscular junction. J. Neurosci. *25*, 3199–3208.

Feldman, D.E. (2012). The spike-timing dependence of plasticity. Neuron *75*, 556–571.

Frank, C.A., Kennedy, M.J., Goold, C.P., Marek, K.W., and Davis, G.W. (2006). Mechanisms underlying the rapid induction and sustained expression of synaptic homeostasis. Neuron *52*, 663–677.

Glanzman, D.L. (2010). Common mechanisms of synaptic plasticity in vertebrates and invertebrates. Curr. Biol. *20*, R31–R36.

Hebb, D.O. (1949). The Organization of Behavior (New York: John Wiley & Sons).

Heine, M., Groc, L., Frischknecht, R., Béïque, J.C., Lounis, B., Rumbaugh, G., Huganir, R.L., Cognet, L., and Choquet, D. (2008). Surface mobility of postsynaptic AMPARs tunes synaptic transmission. Science *320*, 201–205.

Hoang, B., and Chiba, A. (2001). Single-cell analysis of *Drosophila* larval neuromuscular synapses. Dev. Biol. *229*, 55–70.

Kandel, E.R. (2009). The biology of memory: a forty-year perspective. J. Neurosci. *29*, 12748–12756.

Malinow, R., and Malenka, R.C. (2002). AMPA receptor trafficking and synaptic plasticity. Annu. Rev. Neurosci. *25*, 103–126.

Marrus, S.B., and DiAntonio, A. (2004). Preferential localization of glutamate receptors opposite sites of high presynaptic release. Curr. Biol. *14*, 924–931.

Marrus, S.B., Portman, S.L., Allen, M.J., Moffat, K.G., and DiAntonio, A. (2004). Differential localization of glutamate receptor subunits at the *Drosophila* neuromuscular junction. J. Neurosci. *24*, 1406–1415.

Nagel, G., Szellas, T., Huhn, W., Kateriya, S., Adeishvili, N., Berthold, P., Ollig, D., Hegemann, P., and Bamberg, E. (2003). Channelrhodopsin-2, a directly light-gated cation-selective membrane channel. Proc. Natl. Acad. Sci. USA *100*, 13940–13945.

Paradis, S., Sweeney, S.T., and Davis, G.W. (2001). Homeostatic control of presynaptic release is triggered by postsynaptic membrane depolarization. Neuron *30*, 737–749.

Pawlu, C., DiAntonio, A., and Heckmann, M. (2004). Postfusional control of quantal current shape. Neuron *42*, 607–618.

Peled, E.S., and Isacoff, E.Y. (2011). Optical quantal analysis of synaptic transmission in wild-type and rab3-mutant *Drosophila* motor axons. Nat. Neurosci. *14*, 519–526.

Qin, G., Schwarz, T., Kittel, R.J., Schmid, A., Rasse, T.M., Kappei, D., Ponimaskin, E., Heckmann, M., and Sigrist, S.J. (2005). Four different subunits are essential for expressing the synaptic glutamate receptor at neuromuscular junctions of *Drosophila*. J. Neurosci. *25*, 3209–3218.

Rasse, T.M., Fouquet, W., Schmid, A., Kittel, R.J., Mertel, S., Sigrist, C.B., Schmidt, M., Guzman, A., Merino, C., Qin, G., et al. (2005). Glutamate receptor dynamics organizing synapse formation *in vivo*. Nat. Neurosci. *8*, 898–905.

Schmid, A., Hallermann, S., Kittel, R.J., Khorramshahi, O., Frölich, A.M., Quentin, C., Rasse, T.M., Mertel, S., Heckmann, M., and Sigrist, S.J. (2008). Activity-dependent site-specific changes of glutamate receptor composition *in vivo*. Nat. Neurosci. *11*, 659–666.

Schroll, C., Riemensperger, T., Bucher, D., Ehmer, J., Völler, T., Erbguth, K., Gerber, B., Hendel, T., Nagel, G., Buchner, E., and Fiala, A. (2006). Light-induced activation of distinct modulatory neurons triggers appetitive or aversive learning in *Drosophila* larvae. Curr. Biol. *16*, 1741–1747.

Shepherd, J.D., and Huganir, R.L. (2007). The cell biology of synaptic plasticity: AMPA receptor trafficking. Annu. Rev. Cell Dev. Biol. *23*, 613–643.

Sigrist, S.J., Thiel, P.R., Reiff, D.F., Lachance, P.E., Lasko, P., and Schuster, C.M. (2000). Postsynaptic translation affects the efficacy and morphology of neuromuscular junctions. Nature *405*, 1062–1065.

Sigrist, S.J., Reiff, D.F., Thiel, P.R., Steinert, J.R., and Schuster, C.M. (2003). Experience-dependent strengthening of *Drosophila* neuromuscular junctions. J. Neurosci. *23*, 6546–6556.

Steinert, J.R., Kuromi, H., Hellwig, A., Knirr, M., Wyatt, A.W., Kidokoro, Y., and Schuster, C.M. (2006). Experience-dependent formation and recruitment of large vesicles from reserve pool. Neuron *50*, 723–733.

Verstreken, P., and Bellen, H.J. (2002). Meaningless minis? Mechanisms of neurotransmitter-receptor clustering. Trends Neurosci. *25*, 383–385.

Wagh, D.A., Rasse, T.M., Asan, E., Hofbauer, A., Schwenkert, I., Dürrbeck, H., Buchner, S., Dabauvalle, M.C., Schmidt, M., Qin, G., et al. (2006). Bruchpilot, a protein with homology to ELKS/CAST, is required for structural integrity and function of synaptic active zones in *Drosophila*. Neuron *49*, 833–844.